Japanese Journal of Applied Physics **54**, 01AE01 (2015) **REGULAR PAPER**
http://dx.doi.org/10.7567/JJAP.54.01AE01

A study on the etching characteristics of magnetic tunneling junction materials using DC pulse-biased inductively coupled plasmas

Kyung Chae Yang[1], Min Hwan Jeon[2], and Geun Young Yeom[1,2*]

[1]*Department of Advanced Materials Science and Engineering, Sungkyunkwan University, Suwon 440-746, Republic of Korea*
[2]*SKKU Advanced Institute of Nano Technology (SAINT), Sungkyunkwan University, Suwon 440-746, Republic of Korea*

Received February 7, 2014; revised June 14, 2014; accepted June 16, 2014; published online October 29, 2014

The etching properties of magnetic materials composing the magnetic tunnel junction (MTJ) such as CoPt, MgO, CoFeB, and CoPt/MgO/CoFeB were investigated in DC pulse biased CO/NH_3 inductively coupled plasmas (ICPs) and their etch characteristics were compared with those etched by RF CW biased ICPs. The use of DC pulse biased ICPs instead of RF CW biased ICPs improved the etch selectivity of the MTJ materials over W and also decreased the residue on the surface of the etched materials possibly due to the more stable and volatile etch product formation during the DC pulse off time and the enhanced removal of the etch products by mono-energetic ions during the DC pulse on time. When MTJ materials masked with W were etched, more anisotropic etch profile could be also observed when the MTJ materials were etched with the DC pulse biasing of 60% duty percentage compared with those etched with RF CW biasing due to the decreased redeposition of etch products on the sidewall of the etched feature in addition to the enhanced etch selectivity over W.

1. Introduction

A variety of magnetic random access memory (MRAM) technologies has been investigated experimentally over a period of many decades because of the industrial potential in the non-volatile memory markets.[1–3)] The main attributes of MRAM technology are nonvolatile characteristics preserving the memory states even when the power is eliminated from the devices and very large ($>10^{15}$) write/read cycle capability.[1,4,5)] The main difference of memory behavior between the MRAM and static random access memory (SRAM) or dynamic random access memory (DRAM) is that MRAM uses magnetic tunnel junctions (MTJs) as an information carrier rather than an electric charge.[6)] Especially, as the basic of MRAM cell, spin transfer torque (STT) switching-types of MTJs have been investigated intensively these days due to the potential advantages such as fast speed, low operation power, infinite endurance, and high density.[1,7–9)]

However, to satisfy the minimization of the size and shape of MTJs, the precise and anisotropic etching of the MTJ stack is required.[10–12)] For this, an etch process using ion milling method has been initially applied in the etching of the magnetic materials. However, this method is known to exhibit problems in the application to nanoscale MRAM integrated circuit processing due to heavy redeposition on the sidewall of the patterns, lack of selectivity, and slow etch rate.[13–15)] Therefore, plasma etching techniques such as reactive ion etching (RIE), inductively coupled plasma (ICP) etching, etc. have been investigated as alternate techniques in improving these disadvantages.[16–19)] But plasma etching using halogen-based gas such as Cl_2 causes other problem such as corrosion and also causes heavy redeposition on the sidewall of the pattern by chlorine etch compounds even though the higher substrate temperature tends to volatilize the chlorine-based residual etch byproducts by increasing their vapor pressure.[20)] Therefore, many non-corrosive gas combinations such as CO/NH_3, CH_3OH, etc., which are known to form volatile compounds with magnetic materials, have been proposed for the etching of MTJ stacks in recent researches.[21–25)]

However, since the MTJ-related materials such as CoFeB, CoPt, MgO, etc. rarely react to form chemically active species with the plasmas composed of those non-corrosive gas mixtures, many specific etching techniques have been proposed during the etching with the non-corrosive gases. For example, to enhance the volatility of etch products and to obtain good etch profiles, etch techniques such as substrate heating, RF source/bias pulsing, etc. have been proposed.[26,27,29)] Unlike RF CW plasmas, it was reported that, by pulsing the RF source plasmas, independent control of plasma parameters such as plasma potentials, electron temperature, etc. can be achieved.[28)] In the case of the RF bias pulsing, it has found out that stable and volatile compounds can be formed easily during the pulse-off time of the RF bias pulse cycle for higher etch selectivity and less etch residue.[29)] However, RF pulsing may require a specific matching network to apply for the device processing.

DC pulse-biasing instead of RF biasing has been investigated recently in the etching of III–V compounds to etch III–V compounds more selectively over the photoresist and more anisotropically in addition to the advantage of no need for specific matching network, low heat generation during the etching, etc.[30)] In this study, DC pulse biasing was also introduced in the etching of MTJ-related materials to explore the possibility in improving the etch characteristics of the MTJ-related materials such as CoFeB, CoPt, MgO and W using an optimized CO/NH_3 gas mixture and the etch characteristics were compared with those etched by conventional RF CW biasing.

2. Experimental methods

The schematic diagram of the ICP etcher equipment (STS PLC) used in this experiment is shown in Fig. 1. As shown in the figure, the ICP etcher has one-turn copper coil around the ceramic chamber and a 13.56 MHz RF CW source power generator was connected to this coil to generate high density plasmas. A separate DC power generator (ENI RPG100, 10 kW) was connected to the substrate directly through a band pass filter without connecting to any matching network for biasing and to control the ion bombardment energy. For comparison, the substrate was also biased using a conventional 13.56 MHz CW RF power through a matching network. The etch gases were injected through the top of a chamber and the substrate was heated using an oil heater (LAUDA P5).

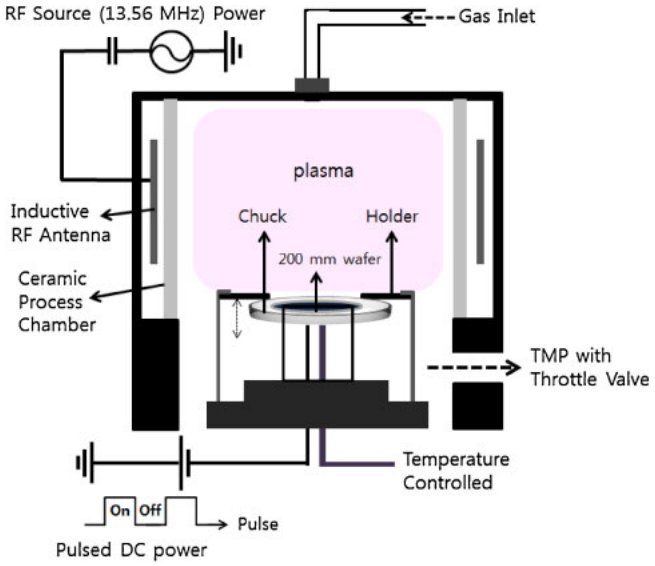

Fig. 1. (Color online) A schematic diagram of the DC pulse biased ICP etching system.

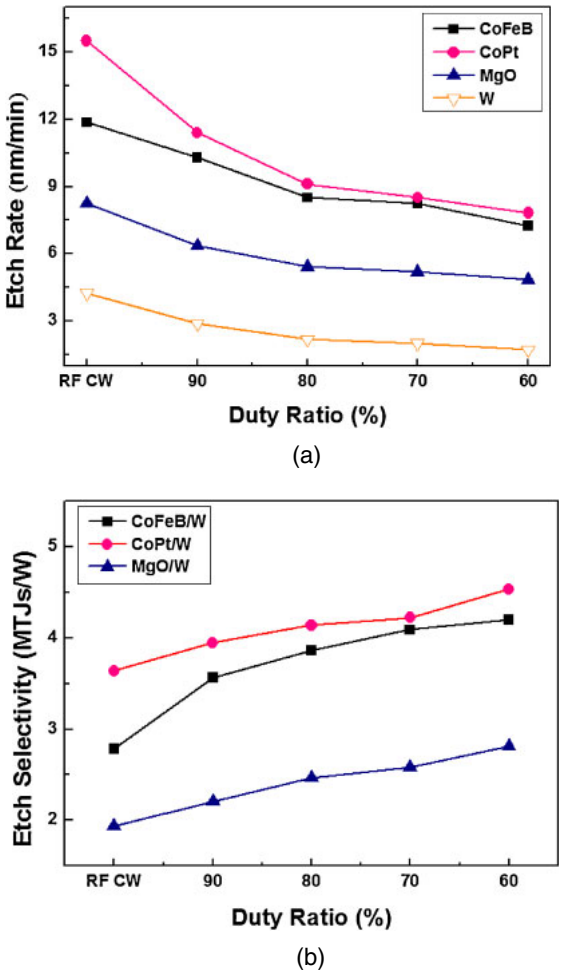

Fig. 2. (Color online) Etch rates of CoFeB, CoPt, MgO, and W and the etch selectivity of CoFeB/W, CoPt/W, MgO/W as a function of DC pulse duty ratio at −300 V of DC pulse voltage and 50 kHz of the pulse frequency using 50 sccm CO/NH_3 gas mixture at a pressure of 5 mTorr, 500 W of 13.56 MHz CW ICP power, and 200 °C of the substrate temperature. (a) Etch rates and (b) etch selectivities as a function of DC pulse duty ratio.

The full stack structure of the MTJs used in this work was consisted of magnetic materials CoPt (10 nm)/MgO (1 nm)/CoFeB (10 nm) and the hardmask material W (100 nm) on the Ta (5 nm)/silicon. Also, blanket unit thin films, such as CoPt, MgO, CoFeB, W were also prepared on the Si wafers with the thickness of about 20 nm using co-sputter deposition. The W hardmask layer was patterned using a SiO_2 pattern on the W before etching the MTJ layer. The dry etching of the CoPt, MgO, CoFeB, and W thin film samples and CoPt/MgO/CoFeB stack samples masked with W was progressed with a CO (12.5 sccm)/NH_3 (37.5 sccm) gas mixture and at the process pressure of 5 mTorr as a function of the DC bias voltage and the duty ratio. The DC pulse bias voltage was varied from −300 to −500 V and the duty ratio was varied from 90 to 60% at the pulse frequency of 50 kHz. During the etching, the substrate was maintained at 200 °C by an oil heater.

After the etching of the blanket unit thin films, the etch depth of the processed sample was measured using a surface profilometer (KLA Tencor Alpha-step 500). Among the etched MTJ-related materials, the thickness and chemical bonding states of the chemically reacted layer formed on the etched CoFeB surfaces were analyzed by X-ray photoelectron spectroscopy (XPS; VG Microtech ESCA2000). Also, the etch profile of MTJ stacks masked with W was observed by field emission scanning electron microscopy (FE-SEM; Hitachi S-4700).

3. Results and discussion

While 13.56 MHz RF power was applied to the ICP source continuously for the dissociation and ionization of CO/NH_3, the power to the substrate for the ion bombardment source was changed from conventional CW RF power to DC pulse power and the effects of DC pulse biasing on the etch characteristics were investigated. Figure 2 shows (a) the etch rates of CoFeB, CoPt, MgO, and W and (b) the etch selectivities of MTJ materials over W measured as a function of duty ratio. The etching was carried out with the ICP RF source power of 500 W using CO (12.5 sccm)/NH_3 (37.5 sccm) at 5 mTorr, and at the substrate temperature of 200 °C. The duty ratio was varied from 90 to 60% at the DC pulse bias voltage of −300 V while keeping the pulse frequency at 50 kHz. The etch rates and the etch selectivities were also compared with those etched using RF CW biasing at −300 V of DC self-bias voltage. As shown in the figure, the etch rates of CoFeB, CoPt, MgO, and W were decreased with decreasing the duty ratio due to the increased pulse off time during the biasing, that is, due to the decrease of high energy ion bombardment time. Therefore, the etch rates of MTJ materials etched by the DC pulse biasing were also lower than those etched by RF CW biasing at −300 V. However, as shown in Fig. 2(b), by decreasing the duty ratio of the DC bias pulsing, the etch selectivities of magnetic materials over W were increased and also the etch selectivities were higher than those by RF CW biasing. The increase of etch selectivity is believed to be related to the increased chemical reaction of dissociated gas mixture with magnetic materials, that is, the formation of volatile carbonyl compounds such as $Co(CO)_x$, $Fe(CO)_x$, etc. for easier sputter removal from the surface by the ion bombardment during the DC bias pulse on time.

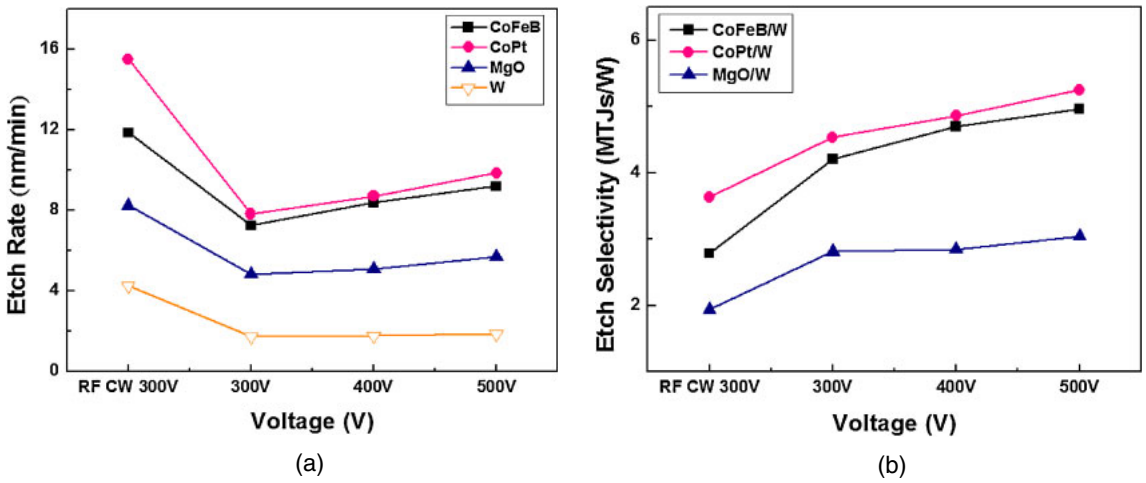

Fig. 3. (Color online) Etch rates of CoFeB, CoPt, MgO, and W and etch selectivity of CoFeB/W, CoPt/W, MgO/W as a function of DC pulse bias voltage at 60% duty ratio. Other conditions are the same as those in Fig. 2: (a) etch rates and (b) etch selectivities as a function of pulsed DC voltage.

Figures 3(a) and 3(b) show the etch rates of MTJ-related materials and the etch selectivities of MTJ materials over W measured as a function of DC pulse bias voltage, respectively. The voltage of the DC pulse power was varied from −300 to −500 V at the pulse duty ratio of 60% and the results were also compared with those etched using RF CW biasing at −300 V. The other operating conditions were the same as those in Fig. 2. As shown in the figure, even though the etch rates of magnetic materials etched by the DC bias pulsing with 60% duty ratio were lower than those etched with RF CW biasing, the etch rates could be improved by increasing the DC pulse bias voltage. In addition, the etch selectivities of the magnetic materials over W were improved with the increase of DC bias voltage possibly due to the increased removal rate of etch products at the higher ion bombardment energy and due to the more selective etching of the magnetic material compounds than W compounds.

To investigate the reason for the high etch selectivities of magnetic materials for DC pulse biasing compared to RF CW biasing at the similar ion bombardment energy, the chemical bonding states of the CoFeB surfaces, as one of the magnetic materials, etched by DC pulse biasing and by RF CW biasing were compared using XPS. Figures 4(a) and 4(b) show the XPS narrow scan data of Co 2p, Fe 2p, and B 1s measured, during the depth profiling of the surface from up to 360 s on the CoFeB surface etched using the RF CW biasing and DC pulse biasing, respectively. −300 V of self-voltage was used for the RF CW biasing and −300 V of DC pulse bias voltage with 60% duty ratio was used. The samples were etched with CO/NH_3 for 3.5 min. Other etch conditions were maintained the same as those in Fig. 2. The depth profiling was conducted with an Ar^+ ion gun of 3 kV ion energy and 2 μA ion current. As shown in the figure, the etched CoFeB showed additional peaks related to metal oxide at 781 and 797.1 eV for Co–O, 710 and 723.5 eV for Fe–O, and 192 eV for B–O in addition to the metallic peaks observed at 778.3 and 793.2 eV for Co 2p, 707 and 720.2 eV for Fe 2p, and 188 eV for B 1s. The additional peaks were decreased with the increase of depth profiling time and, as shown in the figure, the CoFeB etched with DC pulse biasing was recovered at the shorter profiling depth compared to that etched with RF CW biasing.

The composition of the residue on the CoFeB etched using RF CW biasing and DC pulse biasing was also measured during the XPS depth profiling in Fig. 4 and the results are shown in Fig. 5. For the pristine CoFeB, the atomic percentages of CoFeB were Co (49.7%), Fe (35.4%), and B (14.9%). After the etching using CO/NH_3 for 3.5 min, a residue layer was formed on the etched CoFeB surface and the surface was mostly composed of carbon and oxygen. However, the carbon and oxygen contents on the surface were decreased and the metallic components such as Co, Fe, and B were recovered with the increase of depth profiling time. Especially, the CoFeB etched by the DC pulse biasing at 60% duty ratio showed a thinner residue layer compared that etched by the RF CW biasing. For the CoFeB etched by the DC bias pulsing, 22% O and 13% C after 90 s sputtering, 10% O and 4% C after 180 s sputtering, and the complete recovery of CoFeB similar to that of pristine CoFeB after 180 s sputtering were observed. On the other hand, the CoFeB etched by the RF CW biasing showed 35% O and 15% C after 90 s sputtering, 25% O and 7% C after 180 s sputtering, and no complete recovery of CoFeB even after 270 s sputtering. The existence of abundant C and O on the etched magnetic material surface may indicate that the formation of metal carbonyl $(CO)_x$ during the etching as the etch products for the volatile etch compounds even though the peaks related to metal carbonyls could not be identified during the XPS analysis in Fig. 4 due to the similar peak positions, therefore, due to the difficulty in the peak separation between metal peaks and metal carbonyl peaks.[31)]

The decreased residue layer on the etched magnetic material such as CoFeB surface shown in Fig. 5 may also indicate the decreased sidewall redeposited residue during the etching of a masked magnetic materials including CoFeB. To investigate the degree of sidewall residue on the etched MTJ feature composed of CoFeB/MgO/CoPt, the MTJ material masked with W was etched both by DC pulse biasing and by RF CW biasing and the etch profiles were observed by FE-SEM and the results are shown in Fig. 6. The etch conditions are the same as those conditions in Fig. 5.

As shown in the figure, the MTJ etched feature formed by the RF CW biasing showed a sloped etch profile and a thicker feature size while the that formed by the DC pulse

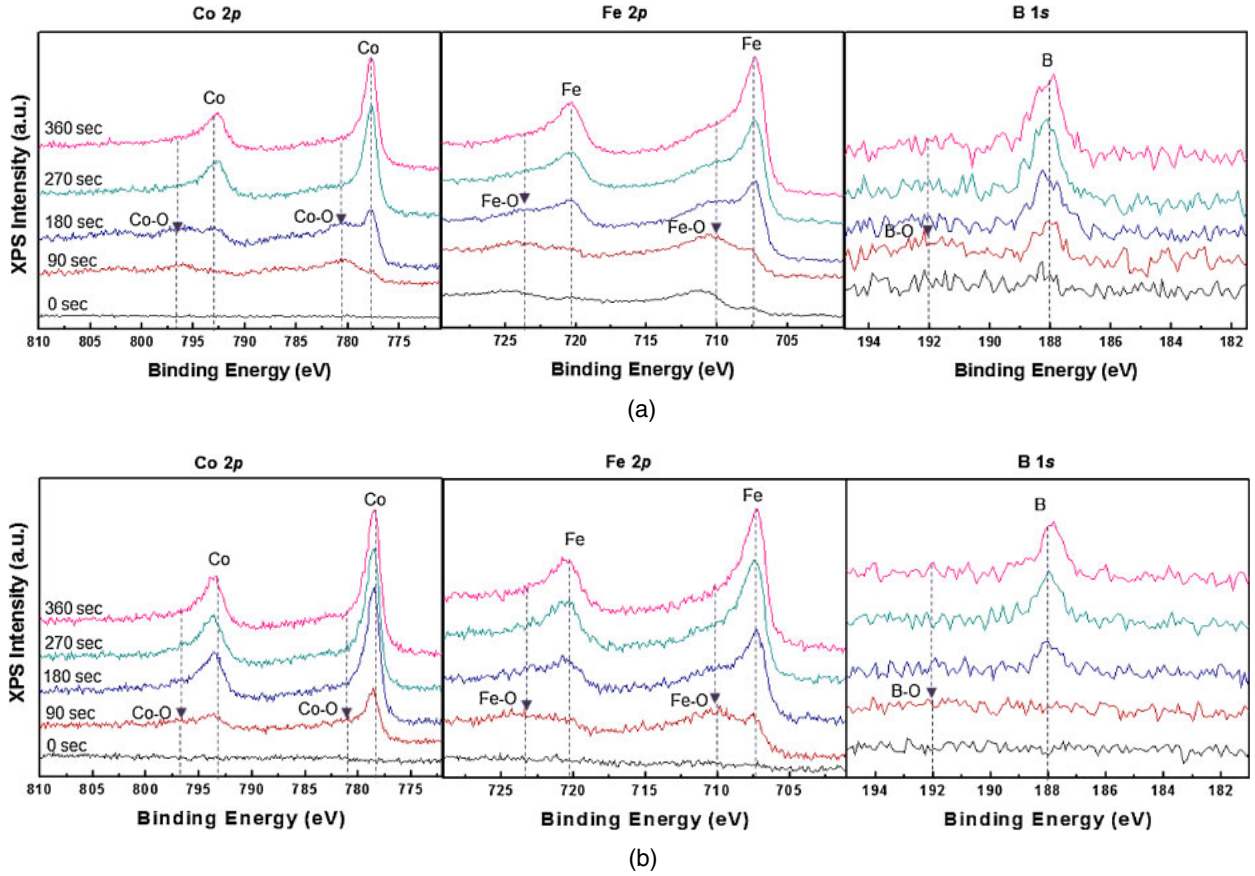

Fig. 4. (Color online) XPS narrow scan peaks of Co 2p, Fe 2p, B 1s, and C 1s of the CoFeB surface etched in the CO/NH_3 plasmas measured during depth profiling: (a) RF CW biasing, (b) DC pulsed biasing at 60% duty ratio. Other etching conditions are the same as those in Fig. 2.

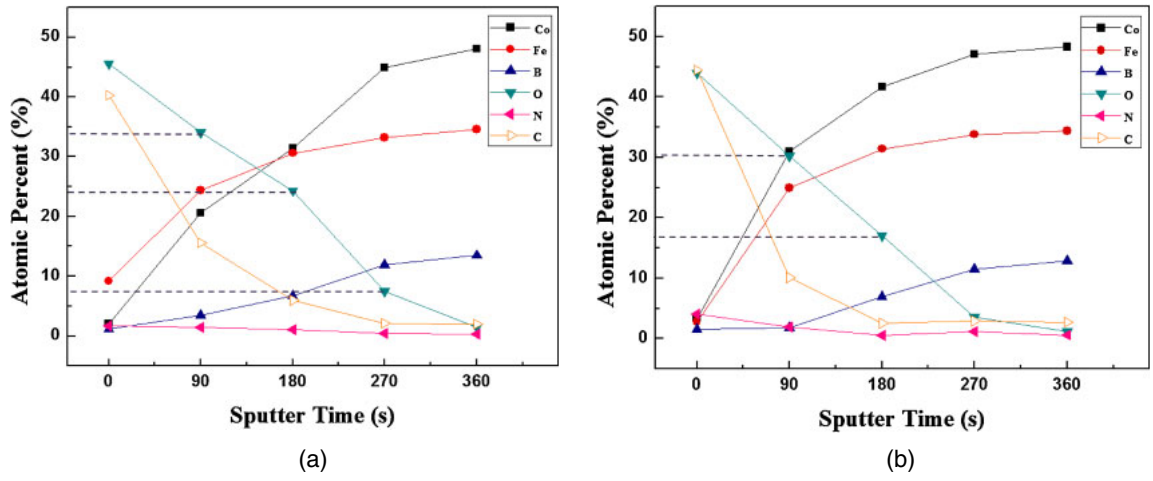

Fig. 5. (Color online) Residue composition on the CoFeB surface measured as a function of XPS depth profiling time: (a) with RF CW biasing and (b) with DC pulse biasing.

biasing showed an anisotropic etch profile and a thinner feature size suggesting the less sidewall redeposition during the etching. In addition, compared to the MTJ feature etched by RF CW biasing, that etched by DC pulsing shows the less faceting of W hardmask possibly due to the lower etch rate of W compared to MTJ materials for DC pulse biasing. The less faceting of W etch profile also appears to improve the MTJ etch profile in addition to the decreased sidewall redeposition.

Figure 7 shows a cartoon showing a possible mechanism of the lower sidewall redeposition and less residue layer for the MTJ material etched by DC pulse biasing compared to those etched by RF CW biasing. In the case of RF CW biasing, the etch products formed on the etched surface of the MTJ materials are more easily redeposited on the sidewall of the etched feature and the bottom surface of the etched material. It is because stable and volatile etch compounds such as metal carbonyl compounds cannot be easily formed

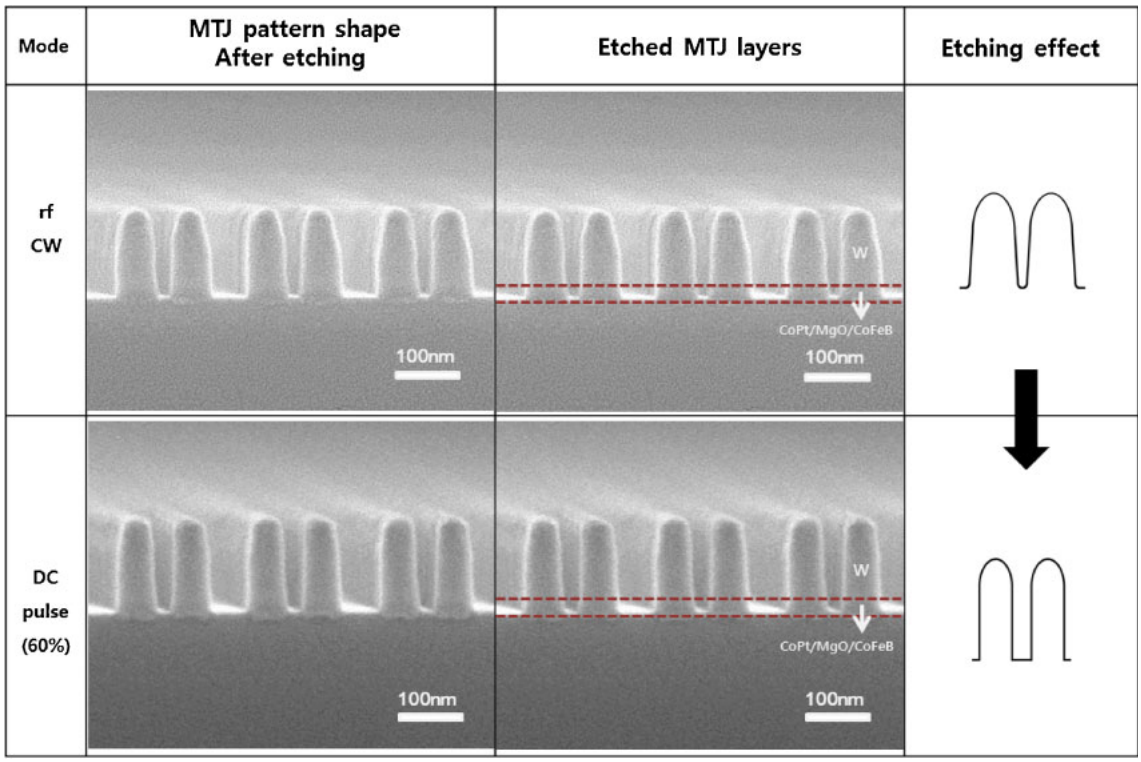

Fig. 6. (Color online) SEM images of the etched MTJ stacks composed of CoFe/MgO/CoPt and masked with W. The MTJ stacks were etched with DC pulse biasing of 60% duty ratio and with RF CW biasing. Other etch conditions are the same as those in Fig. 5.

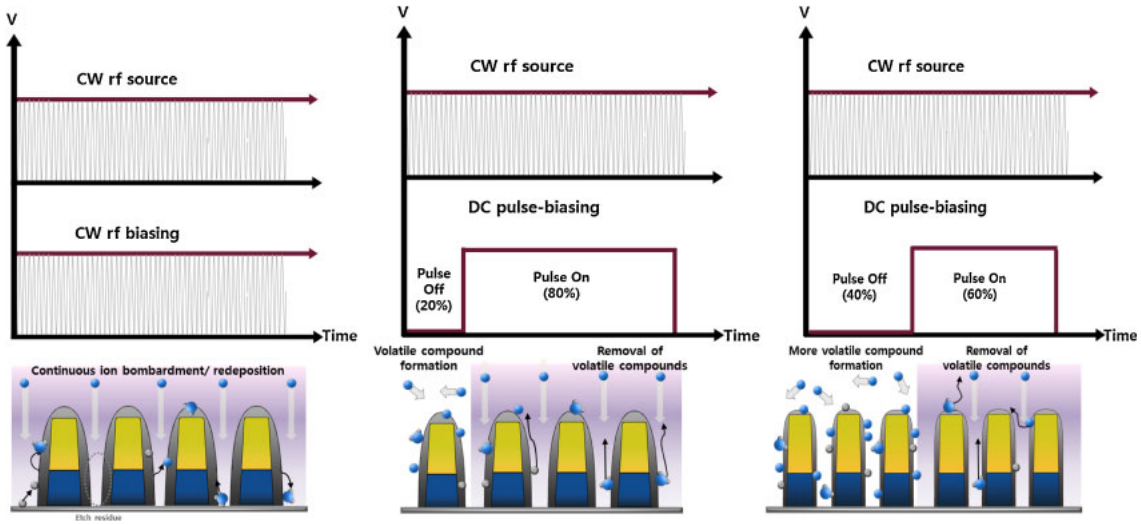

Fig. 7. (Color online) Schematic diagram of etch mechanism for RF CW biasing and DC pulse biasing.

on the surface due to the continuous ion bombardment and dissociation of the etch products during the etching. However, by pulsing the bias power, stable and more volatile etch compounds could be formed during the pulse off time and those compounds can be more easily removed by vaporizing from the surface during the pulse on time without redeposition on the sidewall of the feature. Therefore, more selective etching, less residue on the sidewall and bottom of the etched feature, and highly vertical MTJ etch profile are believed to formed. Similar effects can be also obtained by biasing the substrate using RF pulse biasing. In fact, a previous study[29] showed the improvement of etch selectivities of MTJ material over W, less etch residues, and more anisotropic etch profile by using RF pulse biasing instead of RF CW biasing. However, it is believed that, by using the DC pulse biasing, incident ions can bombard the substrate vertically and with less energy variation by the constant DC voltage on the substrate, that is, with mono-energetic ions during the pulse on time. Therefore, the etch products can be more easily removed from the surface without dissociating metal carbonyl compounds by using a narrow ion energy distribution, and which may lead less sidewall deposition on the etched feature in addition to no difficulties in the matching of pulsed power are required.

4. Conclusions

The etching characteristics of MTJ-related materials such as CoPt, MgO, and CoFeB in DC pulse-biased CO/NH_3 ICPs have been investigated and their etch characteristics were compared with those etched by RF CW biased ICPs. By using DC pulse biasing instead of RF CW biasing, the etch selectivities of the magnetic materials over W were improved and the decrease of DC pulse duty ratio improved the etch selectivity further. The increase of DC bias voltage at a fixed duty ratio also improved the etch selectivity while increasing the etch rates of magnetic materials. The use of DC pulse biasing instead of RF CW biasing also decreased the residue layer thickness on the bottom of the etched magnetic materials. The MTJ (CoPt/MgO/CoFeB) feature etched with DC pulse biasing showed more anisotropic etch profile and less sidewall residue compared to that etched with RF CW biasing. The various improved etch properties of MTJ materials observed with DC pulse biasing appear to be related to the formation of more stable and volatile etch product formation during the DC pulse off time and the enhanced removal of the etch products by mono-energetic ions during the DC pulse on time.

Acknowledgements

The project was supported by the SRC project No. 2011-IN-2219. The authors would like to thank Dr. Satyarth Suri and Dr. Bob Turkot in Intel Corporation for helpful discussion on the MRAM etching.

1) S. S. P. Parkin, K. P. Roche, M. G. Samant, P. M. Rice, R. B. Beyers, R. E. Scheuerlein, E. J. O'Sullivan, S. L. Brown, J. Bucchigano, D. W. Abraham, Y. Lu, M. Rooks, P. L. Trouilloud, R. A. Wanner, and W. J. Gallagher, J. Appl. Phys. **85**, 5828 (1999).
2) S. Tehrani, J. M. Slaughter, E. Chen, M. Durlam, J. Shi, and M. DeHerrera, IEEE Trans. Magn. **35**, 2814 (1999).
3) D. S. Um, D. P. Kim, J. C. Woo, and C. I. Kim, J. Vac. Sci. Technol. A **27**, 818 (2009).
4) S. Tehrani, J. M. Slaughter, M. DeHerrera, B. N. Engel, N. D. Rizzo, J. Salter, M. Durlam, R. W. Dave, J. Janesky, B. Butcher, K. Smith, and G. Grynkewich, Proc. IEEE **91**, 703 (2003).
5) P. P. Freitas, S. Cardoso, R. Sousa, W. Ku, R. Ferreira, V. Chu, and J. P. Conde, IEEE Trans. Magn. **36**, 2796 (2000).
6) G. Sun, X. Dong, Y. Xie, J. Li, and Y. Chen, Proc. IEEE HPCA Symp., 2009, p. 239.
7) D. Apalkov, A. Khvalkovskiy, S. Watts, V. Nikitin, X. Tang, D. Lottis, K. Moon, X. Luo, E. Chen, A. Ong, A. Driskill-Smith, and M. Krounbi, ACM J. Emerg. Technol. Comput. Syst. **9**, 13 (2013).
8) W. S. Zhao, Y. Zhang, T. Devolder, J. O. Klein, D. Ravelosona, C. Chappert, and P. Mazoyer, Microelectron. Reliab. **52**, 1848 (2012).
9) M. Durlam, P. Naji, M. DeHerrera, S. Tehrani, G. Kerszykowski, and K. Kyler, IEEE ISSC Conf. Tech. Dig., 2000, p 130.
10) Y. Otani, H. Kubota, A. Fukushima, H. Maehara, T. Osada, S. Yuasa, and K. Ando, IEEE Trans. Magn. **43**, 2776 (2007).
11) Y. B. Xiao, E. H. Kim, S. M. Kong, and C. W. Chung, Thin Solid Films **519**, 6673 (2011).
12) S. R. Min, H. N. Cho, K. W. Kim, Y. J. Cho, S. H. Choa, and C. W. Chung, Thin Solid Films **516**, 3507 (2008).
13) S. Takahashi, T. Kai, N. Shimomura, T. Ueda, M. Amano, M. Yoshikawa, E. Kitagawa, Y. Asao, S. Ikegawa, T. Kishi, H. Yoda, K. Nagahara, T. Mukai, and H. Hada, IEEE Trans. Magn. **42**, 2745 (2006).
14) K. Sugiura, S. Takahashi, M. Amano, T. Kajiyama, M. Iwayama, Y. Asao, N. Shimomura, T. Kishi, S. Ikegawa, H. Yoda, and A. Nitayama, Jpn. J. Appl. Phys. **48**, 08HD02 (2009).
15) T. Mukai, N. Ohshima, H. Hada, and S. Samukawa, J. Vac. Sci. Technol. A **25**, 432 (2007).
16) B. Shin, I. H. Park, and C. W. Chung, Integrated Ferroelectr. **78**, 233 (2006).
17) S. J. Pearton and D. P. Norton, Plasma Processes Polym. **2**, 16 (2005).
18) T. Y. Lee, I. H. Lee, and C. W. Chung, Thin Solid Films **547**, 146 (2013).
19) T. Kanazawa, S.-I. Motoyama, T. Wakayama, and H. Akinaga, J. Magn. **12**, 81 (2007).
20) H. Maehara, T. Osada, M. Doi, K. Sakamoto, K. Tsunekawa, D. D. Djayaprawira, Y. Kodaira, N. Watanabe, H. Kubota, A. Fukushima, Y. Otani, S. Yuasa, and K. Ando, Dig. IEEE Intermag Conf., 2005, p. 1535.
21) T. Y. Lee, E. H. Kim, and C. W. Chung, Thin Solid Films **521**, 229 (2012).
22) Y. B. Xiao, E. H. Kim, S. M. Kong, and C. W. Chung, Thin Solid Films **519**, 8229 (2011).
23) K. Kinoshita, H. Utsumi, K. Suemitsu, H. Hada, and T. Sugibayashi, Jpn. J. Appl. Phys. **49**, 08JB02 (2010).
24) K. Kinoshita, T. Yamamoto, H. Honjo, N. Kasai, S. Ikeda, and H. Ohno, J. Appl. Phys. **51**, 08HA01 (2012).
25) A. S. Orland and R. Blumenthal, J. Vac. Sci. Technol. B **23**, 1597 (2005).
26) M. Lee and W. J. Lee, Appl. Surf. Sci. **258**, 8100 (2012).
27) K. Watanabe, ECS Trans. **3** [25], 137 (2007).
28) A. Mishra, J. S. Seo, K. N. Kim, and G. Y. Yeom, J. Phys. D **46**, 235203 (2013).
29) M. H. Jeon, H. J. Kim, K. C. Yang, S. K. Kang, K. N. Kim, and G. Y. Yeom, Jpn. J. Appl. Phys. **52**, 05EB03 (2013).
30) J. Y. Shin, K. H. Choi, K. H. Noh, D. K. Park, K. Y. Sohn, G. S. Cho, H. J. Song, J. W. Lee, and S. J. Pearton, Thin Solid Films **521**, 245 (2012).
31) D.-X. Ye, S. Pimanpang, C. Jezewski, F. Tang, J. J. Senkevich, G.-C. Wang, and T.-M. Lu, Thin Solid Films **485**, 95 (2005).